

Jumping Jupiter can explain Mercury's orbit

Fernando Roig

Observatório Nacional, Rua Gal. Jose Cristino 77, Rio de Janeiro, RJ 20921-400, Brazil

froig@on.br

David Nesvorný

Southwest Research Institute, 1050 Walnut St., Suite 300, Boulder, CO 80302, USA

davidn@boulder.swri.edu

Sandro Ricardo DeSouza

Observatório Nacional, Rua Gal. Jose Cristino 77, Rio de Janeiro, RJ 20921-400, Brazil

sandroricardo@on.br

Received _____; accepted _____

Submitted to Astrophysical Journal Letters

Abstract

The orbit of Mercury has large values of eccentricity and inclination that cannot be easily explained if this planet formed on a circular and coplanar orbit. Here, we study the evolution of Mercury’s orbit during the instability related to the migration of the giant planets in the framework of the jumping Jupiter model. We found that some instability models are able to produce the correct values of Mercury’s eccentricity and inclination, provided that relativistic effects are included in the precession of Mercury’s perihelion. The orbital excitation is driven by the fast change of the normal oscillation modes of the system corresponding to the perihelion precession of Jupiter (for the eccentricity), and the nodal regression of Uranus (for the inclination).

Subject headings: planets and satellites: dynamical evolution and stability – planets and satellites: terrestrial planets – planets and satellites: individual (Mercury)

1. Introduction

The orbit of Mercury is the most peculiar among the Solar System planets. It has the largest mean eccentricity and inclination ($e = 0.17$ and $I = 7^\circ$ with respect to the invariable plane), its perihelion longitude ϖ is significantly affected by relativistic effects ($\delta\dot{\varpi} \sim 0.43'' \text{ yr}^{-1}$), and its orbit displays the most chaotic long term dynamics (Laskar 1994). Secular variations have typical amplitudes of $\Delta e \simeq \pm 0.08$ and $\Delta I \simeq \pm 3^\circ$ that are not large enough to explain the current mean values of e and I assuming that Mercury, as well as the other terrestrial planets, ended the formation process on nearly circular and coplanar orbits.

Ward et al. (1976) proposed that the high e, I of Mercury could be produced by the oblateness perturbation of the Sun. An initially large value of the second degree harmonic J_2 caused by a rapidly rotating Sun and its subsequent spin down, would drive the perihelion and node of Mercury into secular resonances with the perihelion and node of Venus, respectively, that would excite the corresponding proper modes of Mercury's orbit. However, recent observational evidence indicate that, by the time the terrestrial planets are in their final stages of formation (~ 30 to 200 Myr depending on the model), the Sun's rotation would be only a few times faster than the current rotation (Bouvier 2013). Moreover, contraction of the star along the pre-main-sequence track occurs on the Kelvin-Helmholtz timescale (~ 30 Myr for the Sun), implying that the J_2 term would be already small when the terrestrial planets are formed.

Laskar (2008), Laskar & Gastineau (2009), and Boué et al. (2012) showed that the chaotic evolution of the orbit of Mercury may lead to large changes of e, I over the age of the Solar System. According to Laskar (2008), the probability of changing Mercury's eccentricity by more than 0.1 over 5 Gyr of evolution is less than 20%. The probability of changing the inclination by more than 5° over the same time scale is even smaller, less

than 10%. Therefore, typically the chaotic variations of Mercury’s orbit do not appear to be able to provide the required excitation in e and I from initially circular and coplanar orbits. In particular, Laskar & Gastineau (2009) performed about 2500 simulations and in none of them was Mercury able to reach an eccentricity smaller than ~ 0.05 over 5 Gyr of evolution, implying that there would be no apparent connection between initially circular orbits and chaotic diffusion over Gyr time scales. Nevertheless, this mechanism cannot be totally ruled out, because we cannot discard the possibility that the initial orbit of Mercury had some eccentricity.

Here, we investigate the possibility that the high eccentricity and inclination of Mercury originated during the instability related to the migration of the giant planets, in the framework of the so-called “jumping Jupiter” model. The giant planets in the Solar System did not form on their current orbits but suffered two types of migration. The first one was gas driven migration (Masset & Snellgrove 2001), which acted on planets during the earliest stages when the nebular gas disk was still present in the system. The present paradigm of this type of migration is provided by the Grand Tack model (Walsh et al. 2011). The second one was planetesimal driven migration (Fernandez & Ip 1984), caused by the gravitational interaction of the giant planets with the disk of planetesimals that remained beyond the orbit of Neptune, once the gas has totally dissipated. Its current paradigm is given by the Nice model (Tsiganis et al. 2005). According to the standard scenario, the terrestrial planets started their formation during the gas nebula phase and are completely formed after ~ 100 Myr (e.g. Chambers & Wetherill 1998). Therefore, the orbital architecture of the inner planets provides important constraints on both migration models. For example, the terrestrial planet system is extremely sensitive to the secular evolution of the giant planets (Brasser et al. 2009; Agnor & Lin 2012; Brasser et al. 2013; Kaib & Chambers 2015), and in particular, a slow and smooth migration of the outer planets would destabilize the orbits of the inner planets.

We focus here on a variant of the Nice model, known as the jumping Jupiter model (Morbidelli et al. 2009). The present version of this model assumes that the system of giant planets was initially constituted of five bodies: Jupiter, Saturn, and three ice giants. During the planetesimal driven migration, the system temporarily develops an instability phase involving mutual close encounters between planets, which ends up by the ejection of one of the ice giants after an encounter with Jupiter (Nesvorný 2011). This makes Jupiter jump inwards while Saturn jumps outwards, and the period ratio between Jupiter and Saturn changes nearly instantaneously from an initial value of ~ 1.5 to the current ~ 2.5 . This model has several advantages (Nesvorný & Morbidelli 2012) over the models of smooth planetesimal driven migration, and has had a great success in reproducing the dynamical properties of several minor bodies populations (Nesvorný et al. 2013, 2014; Deienno et al. 2014; Nesvorný 2015; Morbidelli et al. 2015; Roig & Nesvorný 2015; Brasil et al. 2016).

The role of the giant planet evolution on the formation of the terrestrial planets has been addressed in several recent works (Levison & Agnor 2003; Walsh & Morbidelli 2011; Lykawka & Ito 2013; Jacobson & Morbidelli 2014; Izidoro et al. 2015). Most of these studies focus on forming the terrestrial planets with the right mass and at the right distance from the Sun, but give less attention to their orbital eccentricities and inclinations. In some cases, Mercury is not even taken into account in the models. Although the field is under continuous improvement (for a review see Raymond et al. 2014), the formation of terrestrial planets is still a poorly understood process, and the current models do not constrain well the final orbits. Nevertheless, we know that circularization and alignment of the orbital planes should be expected as a result of dynamical friction during the accretion of the planetary embryos in a disk of planetesimals (Kokubo 2005; O’Brien et al. 2006; Morishima et al. 2008). We also know that the terrestrial planets are not expected to suffer any migration process during or after their formation (Minton & Levison 2014).

In this paper, we present results on the evolution of the terrestrial planets in the jumping Jupiter model, with particular focus on Mercury’s orbit. Our main assumption is that the terrestrial planets were completely formed on nearly circular and coplanar orbits before the occurrence of the giant planets instability. The terrestrial orbits lie initially on the invariable plane of the giant planets. Our goal is to measure the effects of the instability on the orbit of Mercury, and to assess the main mechanisms that are responsible for those effects. In the following sections, we describe the methods (sect. 2), present the results (sect. 3), and give our conclusions (sect. 4).

2. Methods

We have performed a series of numerical simulations of the evolution of the Solar System planets during the jumping Jupiter instability. The system of giant planets is initially constituted of Jupiter, Saturn and three Neptune-size planets, located in a mutual resonant configuration that is the supposedly outcome of the previous gas driven migration phase (Pierens et al. 2014). In particular, Jupiter and Saturn are locked in the 3:2 mean motion resonance, with Jupiter slightly outside of its present orbit. The initial osculating values of semimajor axis a , eccentricity e , and inclination I are shown in Table 1.

The five giant planets migrate according to different evolutions previously obtained in Nesvorný & Morbidelli (2012). These authors performed realistic simulations of migration, where the giant planets interact with a massive disk of planetesimals initially located beyond the outermost planet. The different evolutions arise from different parameters of the planetesimal disk that they considered. In their simulations, Nesvorný & Morbidelli (2012) stored the planets’ positions and velocities in a file at 1 yr intervals over a total time span of 10 Myr. We have not reproduced these simulations; rather we have mimicked the migration by reading the stored positions and interpolating them using the approach described in

Nesvorný et al. (2013). The particular cases analyzed here produce interactions with the ejected ice giant that make the other giant planets to experience a few radial jumps. The net inwards jump of Jupiter is ~ 0.3 AU, and the instability occurs about ~ 6 Myr after the start of the simulations.

In our simulations, the terrestrial planets are initially located at their present mean distances from the Sun, but in almost circular and coplanar orbits. Although this might have not been the actual case, because the early terrestrial planets orbits might have been somewhat excited, we adopt this assumption because we want to isolate the effects of the jumping Jupiter evolution from the effects related to specific initial conditions. The adopted orbital values are shown in Table 1. The remaining orbital elements, namely longitude of node Ω , longitude of perihelion ϖ , and mean longitude λ have been chosen at random between 0° and 360° . For each migration case of the giant planets, we generated 100 different sets of initial conditions for the terrestrial planets with different values of Ω , ϖ , λ .

The simulations have been carried out using an hybrid version of the SWIFT_MVS symplectic integrator that interpolates the stored planetary positions of the giant planets to the desired time step, and propagates the terrestrial planets taking into account their mutual perturbations and the perturbations from the giant planets. In this approach, the terrestrial planets do not perturb the giant ones. Relativistic corrections to Mercury’s orbit have been introduced by an additional acceleration term as in Quinn et al. (1991). The integration time step was 0.01 yr, and the total time span of each simulation was 10 Myr. For a few instability cases, we have performed simulations over much longer time spans (up to 100 Myr) that do not change our main results and conclusions.

It is worth recalling that all the instability evolutions considered here satisfy the constraints defined in Nesvorný & Morbidelli (2012), namely, the final orbits of the outer planets are similar to the real orbits. For example, the proper mode in Jupiter’s eccentricity

is excited to its present value by the planetary encounters. All the evolutions also satisfy the terrestrial planets constraint in that Jupiter’s orbit discontinuously evolves during planetary encounters. This is needed to avoid secular resonances with the terrestrial planets, which would otherwise lead to a disruption of the terrestrial planets system (Brasser et al. 2009; Walsh & Morbidelli 2011).

3. Results

Figure 1 shows the results of our simulations for one specific case of the jumping Jupiter instability. Other instability cases produce similar results, although those of Fig. 1 provide best fits to Mercury’s orbit without degrading the fits to the other terrestrial planets. Moreover, the specific instability case considered in Fig. 1 has also been successfully tested against the constraints of the various minor bodies populations (Nesvorný et al. 2013; Deienno et al. 2014; Nesvorný et al. 2014; Nesvorný 2015; Roig & Nesvorný 2015). In the runs including the relativistic corrections (blue dots in Fig. 1), Mercury’s eccentricity reached final mean values of ~ 0.2 that are very close to the present value of 0.17.

It is worth noting that in all the instability cases considered in this study, we found that Mercury’s eccentricity and inclination always become less excited when relativistic effects are taken into account than when these effects are ignored (cf. blue dots *vs.* red dots in Fig. 1). This happens because general relativity speeds up the precession frequency g_1 of Mercury’s perihelion. Faster values of g_1 make resonances with the perihelion frequency of Jupiter, g_5 , to become less strong by reducing their effective widths, and this leads to less excited final eccentricities. In principle, the relativistic corrections do not introduce any direct drift on the regression frequency s_1 of Mercury’s node, but they produce an indirect effect that also leads to less excited inclinations. A similar result, but in a different context, has been pointed out by Laskar (2008), who found that including relativistic effects in the

long term dynamics simulations of the Solar System planets led to a more bounded chaotic evolution of the orbit of Mercury over Gyr time scales.

We verified that the excitation of Mercury’s eccentricity is driven by the fast sweeping of the linear secular resonance $g_1 - g_5$, in agreement with previous studies (e.g. Brasser et al. 2009). This is illustrated in Fig. 2 for one of the simulations with relativistic corrections shown in Fig. 1. The raise of Mercury’s e is accompanied by the libration of the angle $\varpi_1 - \varpi_5$ over a short period of time. The value of g_5 shows significant variations before the instability (Fig. 2c), but after Jupiter jumps (Fig. 2d) it stabilizes and approaches the value of g_1 , driving the system into a temporary resonance capture. We recall that permanent capture does not happen in this context because the adiabatic threshold is broken as a consequence of the discontinuous evolution of the giant planets.

Figure 3a shows the evolution of the inclination of Mercury in the same simulation of Fig. 2, together with the evolution of the angles $\Omega_1 - \Omega_7$ and $\Omega_1 - \Omega_2$, where the index $_2$ refers to Venus and $_7$ to Uranus (Fig. 3b,c). We find that the inclination suffers two different excitation processes, both related to secular resonances involving the frequency of Mercury’s longitude of node, s_1 . The first one is related to a temporary capture in the $s_1 - s_2$ secular resonance with Venus’ node before the instability. The corresponding resonant angle, $\Omega_1 - \Omega_2$, librates around 0° and the inclination is slightly excited by $\sim 2^\circ$. The main excitation event occurs immediately after the instability, and is related to a temporary capture in the $s_1 - s_7$ secular resonance with Uranus’ node. The corresponding resonant angle, $\Omega_1 - \Omega_7$, librates around 180° and the inclination is strongly excited up to $\sim 9^\circ$, very similar to the present value of 7° . The evolution of the secular frequencies s_1 and s_7 is shown in Fig. 3d, together with the evolution of Uranus semimajor axis (Fig. 3e). We can see that the jump of Uranus from ~ 11 to ~ 17 AU approaches the value of s_7 to that of s_1 , once again driving the system into a temporary resonance capture. It is possible that

the excitation of Mercury’s inclination actually arises from the indirect effect of the s_7 mode in the orbit of Venus (which has an important secular coupling with Mercury; Batygin et al. 2015) or Jupiter, rather than from the direct effect of the s_7 mode in the orbit of Mercury. Unfortunately, we cannot confirm this because the motion during and immediately after the instability is extremely irregular, and a Fourier analysis of the time series is useless to assess the role of the different oscillation modes. It is worth noting, however, that during this last excitation event, the system remains captured in the $s_1 - s_2$ resonance, leading to a nodal coupling between Mercury, Venus, and Uranus.

In general, the instability models analyzed here also provide reasonably good fits to the other terrestrial planets. The eccentricities and inclinations of Venus and the Earth are very well reproduced, as well as the eccentricity of Mars. Final mean values always lie within the range of secular variations. In a few models, the eccentricity of Venus and the Earth are slightly more excited than required, but never above the corresponding secular maxima. The mean inclination of Mars is usually underestimated by some 2° - 3° , but never below the corresponding secular minimum.

We have also tested the final configurations using Fourier analysis to verify if the secular architecture of the planets was correctly reproduced. This has been carried out through a short numerical integration of the final state of the planets, with no migration. We found that all the secular proper frequencies are correctly reproduced. Mercury’s eccentricity and inclination are mainly contributed by the e_{11} and I_{11} modes (i.e. the proper modes), respectively, as it is in the present solar system. The other planets display the same behavior, as expected, although some proper modes have slightly different amplitudes, that differ from the current ones by less than 30% in most cases, and up to a factor of two in the worst case.

4. Conclusions

Our results allows us to conclude that the jumping Jupiter instability can produce the presently large values of eccentricity and inclination of Mercury, even in the extreme case when it is assumed that this planet formed in a circular and coplanar orbit. We tested different instability models and some of them produces final orbits that fit very well to the current orbit of Mercury, while also keeping a good fit to the remaining planets, in terms of both orbital elements and secular architecture. We found that the excitation in Mercury's eccentricity is driven by the oscillation mode of the perihelion frequency of Jupiter, g_5 , while the excitation in inclination is driven by oscillation mode of the node frequency of Uranus, s_7 . We also found that the relativistic correction of the perihelion frequency of Mercury, g_1 , has to be included in the model in order to avoid excessive excitation of Mercury's eccentricity and inclination. The jumping Jupiter evolution provides a more robust model than conservative chaotic evolution, since it not only explains the transition of Mercury from nearly circular and coplanar orbit to the present state, but also fulfills several other constraints imposed by the many populations of solar system objects.

We wish to thank an anonymous referee for his/her helpful comments and criticism. This work has been supported by the Brazilian National Research Council (CNPq) through fellowship 312292/2013-9 and grant 401905/2013-6 within the Science Without Borders Program, and by NASA's Emerging Worlds program. Simulations has made use of the cluster of the Department of Astronomy of the National Observatory of Rio de Janeiro, acquired through CAPES grant 23038.007093/2012-13

REFERENCES

- Agnor, C. B., & Lin, D. N. C. 2012, *ApJ*, 745, 143
- Batygin, K., Morbidelli, A., & Holman, M. J. 2015, *ApJ*, 799, 120
- Boué, G., Laskar, J., & Farago, F. 2012, *A&A*, 548, A43
- Bouvier, J. 2013, in *EAS Publications Series*, Vol. 62, *EAS Publications Series*, ed. P. Hennebelle & C. Charbonnel, 143–168
- Brasil, P. I. O., Roig, F., Nesvorný, D., et al. 2016, *Icarus*, 266, 142
- Brasser, R., Morbidelli, A., Gomes, R., Tsiganis, K., & Levison, H. F. 2009, *A&A*, 507, 1053
- Brasser, R., Walsh, K. J., & Nesvorný, D. 2013, *MNRAS*, 433, 3417
- Chambers, J. E., & Wetherill, G. W. 1998, *Icarus*, 136, 304
- Deienno, R., Nesvorný, D., Vokrouhlický, D., & Yokoyama, T. 2014, *AJ*, 148, 25
- Fernandez, J. A., & Ip, W.-H. 1984, *Icarus*, 58, 109
- Izidoro, A., Raymond, S. N., Morbidelli, A., & Winter, O. C. 2015, *MNRAS*, 453, 3619
- Jacobson, S. A., & Morbidelli, A. 2014, *Phil. Trans. Roy. Soc. A*, 372, 30174
- Kaib, N. A., & Chambers, J. E. 2015, *ArXiv e-prints*, arXiv:1510.08448
- Kokubo, E. 2005, in *IAU Colloq. 197: Dynamics of Populations of Planetary Systems*, ed. Z. Knežević & A. Milani, 41–46
- Laskar, J. 1994, *A&A*, 287, L9
- . 2008, *Icarus*, 196, 1

- Laskar, J., & Gastineau, M. 2009, *Nature*, 459, 817
- Levison, H. F., & Agnor, C. 2003, *AJ*, 125, 2692
- Lykawka, P. S., & Ito, T. 2013, *ApJ*, 773, 65
- Masset, F., & Snellgrove, M. 2001, *MNRAS*, 320, L55
- Minton, D. A., & Levison, H. F. 2014, *Icarus*, 232, 118
- Morbidelli, A., Brasser, R., Tsiganis, K., Gomes, R., & Levison, H. F. 2009, *A&A*, 507, 1041
- Morbidelli, A., Walsh, K. J., O’Brien, D. P., Minton, D. A., & Bottke, W. F. 2015, *ArXiv e-prints*, arXiv:1501.06204
- Morishima, R., Schmidt, M. W., Stadel, J., & Moore, B. 2008, *ApJ*, 685, 1247
- Nesvorný, D. 2011, *ApJ*, 742, L22
- . 2015, *AJ*, 150, 68
- Nesvorný, D., & Morbidelli, A. 2012, *AJ*, 144, 117
- Nesvorný, D., Vokrouhlický, D., & Deienno, R. 2014, *ApJ*, 784, 22
- Nesvorný, D., Vokrouhlický, D., & Morbidelli, A. 2013, *ApJ*, 768, 45
- O’Brien, D. P., Morbidelli, A., & Levison, H. F. 2006, *Icarus*, 184, 39
- Pierens, A., Raymond, S. N., Nesvorný, D., & Morbidelli, A. 2014, *ApJ*, 795, L11
- Quinn, T. R., Tremaine, S., & Duncan, M. 1991, *AJ*, 101, 2287
- Raymond, S. N., Kokubo, E., Morbidelli, A., Morishima, R., & Walsh, K. J. 2014, in *Protostars and Planets VI*, ed. H. Beuther, R. S. Klessen, C. P. Dullemond, & T. Henning, 595–618

Roig, F., & Nesvorný, D. 2015, *AJ*, 150, 186

Tsiganis, K., Gomes, R., Morbidelli, A., & Levison, H. F. 2005, *Nature*, 435, 459

Walsh, K. J., & Morbidelli, A. 2011, *A&A*, 526, A126

Walsh, K. J., Morbidelli, A., Raymond, S. N., O’Brien, D. P., & Mandell, A. M. 2011, *Nature*, 475, 206

Ward, W. R., Colombo, G., & Franklin, F. A. 1976, *Icarus*, 28, 441

Table 1: Initial Orbital Elements and Masses of the Planets.

Planet	Mass (M_{Jup})	a (AU)	e	I ($^\circ$)
Mercury	0.00017	0.387	0.001	0.01
Venus	0.00256	0.723	0.001	0.01
Earth	0.00318	1.000	0.001	0.01
Mars	0.00034	1.524	0.001	0.01
Jupiter	1.00000	5.469	0.003	0.05
Saturn	0.29943	7.457	0.011	0.02
Ice #1	0.05307	10.108	0.017	0.11
Ice #2	0.05307	16.080	0.006	0.07
Ice #3	0.05411	22.172	0.002	0.05

Fig. 1.— The terrestrial planets orbits in an example of jumping Jupiter evolution. Red dots are the final mean values of 400 fictitious orbits (100 orbits per planet), when no relativistic correction is applied to Mercury’s orbit. Blue dots are similar results, but applying the relativistic correction. The final values are averages over the last 1 Myr of evolution. The initial conditions of the fictitious orbits are represented by the small black dots at $e \simeq 0$, $I \simeq 0$. Open triangles give the current mean values of the orbital elements, and error bars give their secular variations (maximum and minimum excursions of the elements) over 5 Myr.

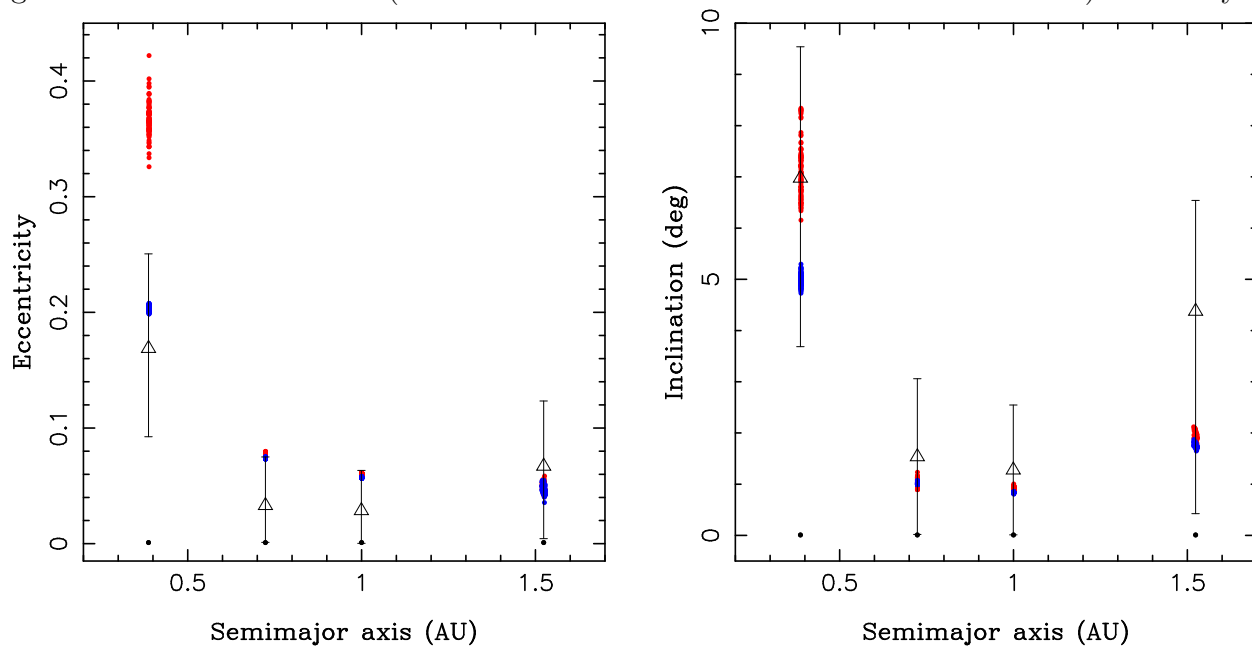


Fig. 2.— Evolution of: (a) the eccentricity of Mercury; (b) the secular angle $\varpi_1 - \varpi_5$; (c) the secular frequencies of the perihelion of Mercury (crosses) and Jupiter (circles); and (d) the semimajor axis of Jupiter. The jumping Jupiter instability occurs between 5.71 and 5.74 Myr (vertical dashed line). The excitation of Mercury’s eccentricity up to ~ 0.2 is related to a temporary trapping in the linear secular resonance $g_1 - g_5$ between the perihelia of Mercury and Jupiter. In panel (c), the secular frequencies have been numerically computed from the corresponding ϖ time series, over windows of 0.1 Myr in width.

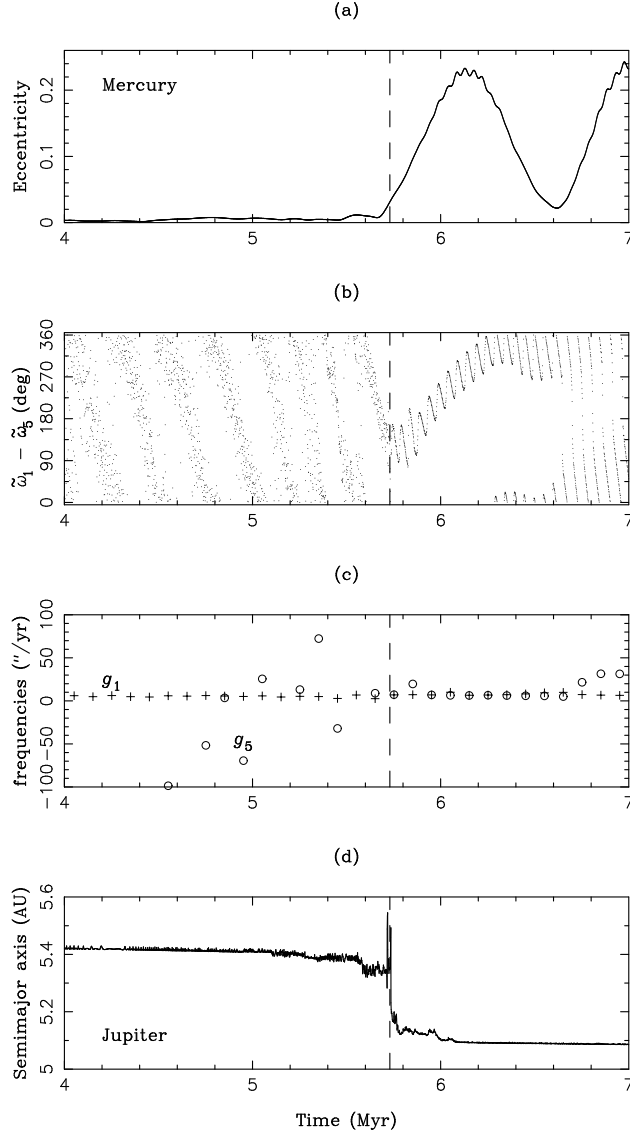


Fig. 3.— Evolution of: (a) the inclination of Mercury; (b) the secular angle $\Omega_1 - \Omega_7$; (c) the secular angle $\Omega_1 - \Omega_2$; (d) the secular frequencies of the nodes of Mercury (crosses) and Uranus (circles); and (e) the semimajor axis of Uranus. The jumping Jupiter instability is indicated by the vertical dashed line. The excitation of Mercury’s inclination up to $\sim 9^\circ$ is related to a temporary trapping in the linear secular resonance $s_1 - s_7$ between the nodes of Mercury and Uranus. Before the instability, a slight excitation up to 2° is related to a secular resonance with the node of Venus. In panel (d), the secular frequencies have been numerically computed from the corresponding Ω time series, over windows of 0.1 Myr in width.

Fig. 3.—

